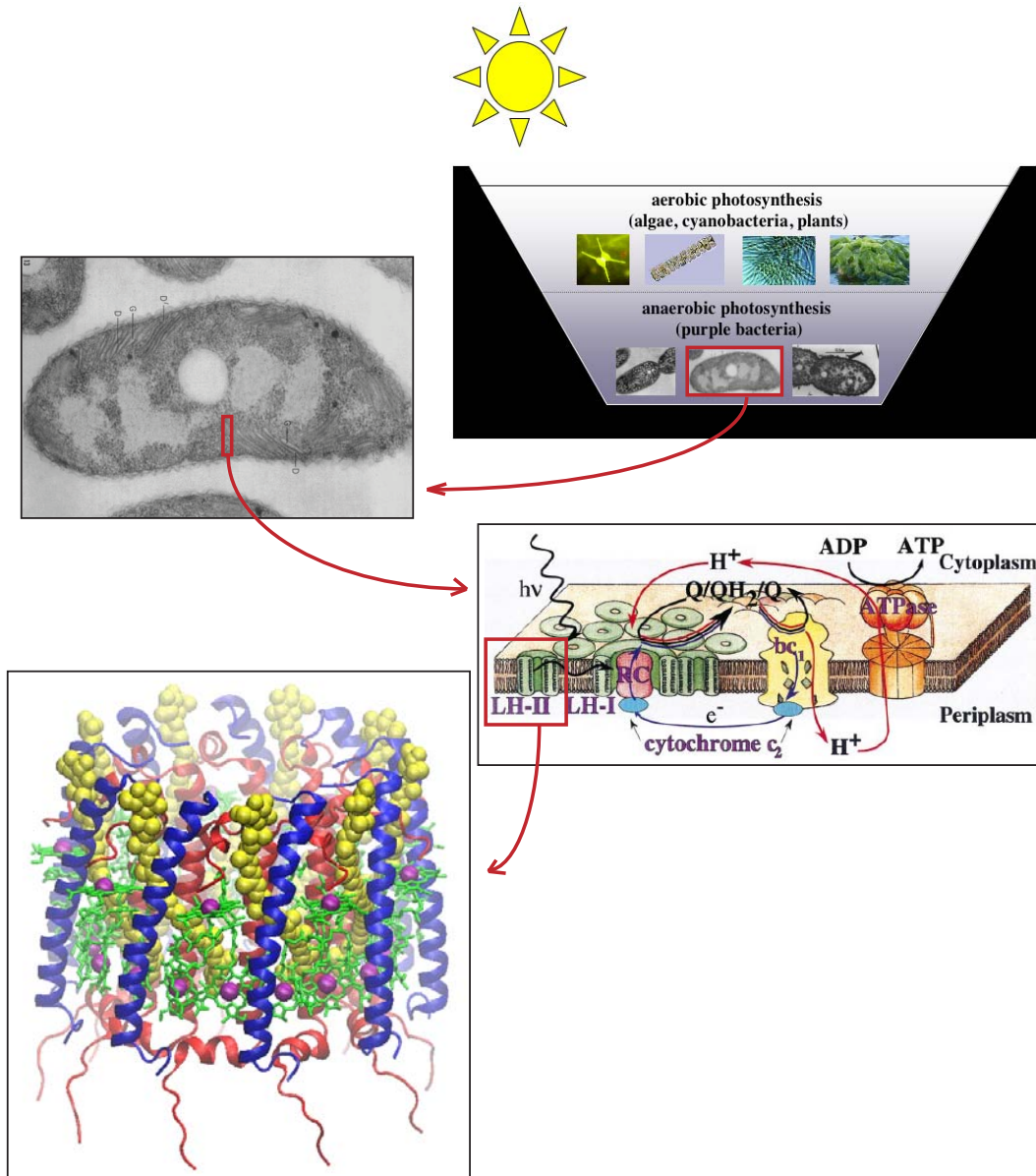


Case Study: Light Harvesting Complex II

Danielle Chandler, Jen Hsin and James C. Gumbart



Cover Figure: Purple bacteria live at the bottom of ponds or lakes, and some purple bacteria can harvest light and produce energy through photosynthesis. Their photosynthetic apparatus are found inside the bacterial membrane, consisting of several proteins. One of these proteins is the ring-like Light Harvesting Complex II, the protein investigated in this case study.

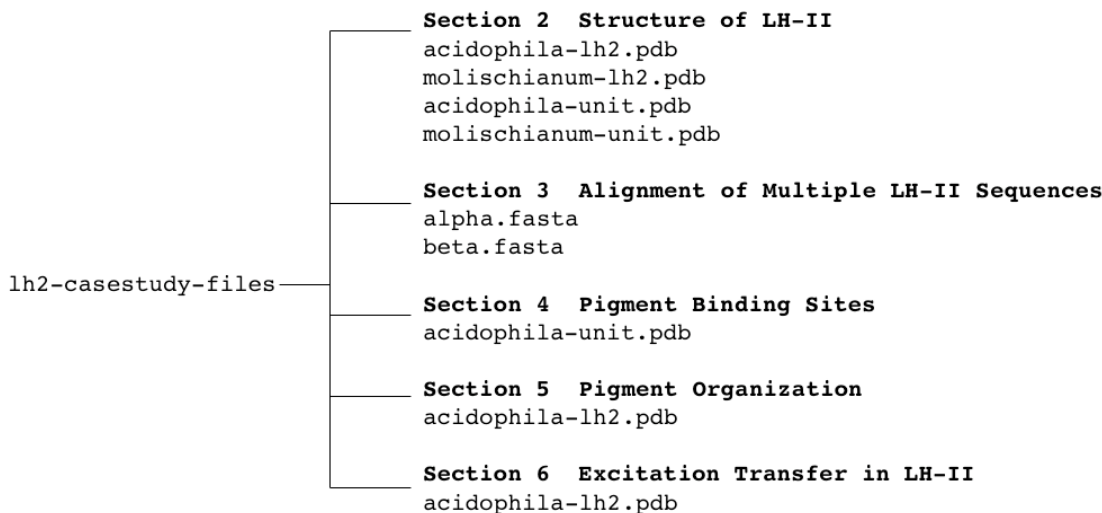


Figure 1: The required files for each section of this case study. All files can be found in the lh2-casestudy-files folder.

1 Introduction

Sunlight is ultimately the energy source for nearly all life on Earth. Many organisms, such as plants, algae, and some bacteria, have developed a means to harvest sunlight and turn it into chemical energy, a process known as photosynthesis. Photosynthesis occurs with an amazingly high efficiency, not surprising given the more than 3.5 billion years of evolution [1]. Among all photosynthetic organisms, purple bacteria are considered to have the oldest, and hence the most simple, photosynthetic apparatus, making them ideal candidates for photosynthetic studies [2]. Although purple bacteria are not as structurally complex as other more evolutionarily advanced organisms, the photosynthetic process is very similar in principle.

In purple bacteria, just a handful of proteins along with a few cofactors (such as the pigment molecules bacteriochlorophylls and carotenoids) are needed to turn light into chemical energy. Three of these proteins directly harvest sunlight. Light is most often first absorbed by an antenna protein called the Light Harvesting Complex II (LH-II); LH-II then transfers its energy to the nearby protein Light Harvesting Complex I (LH-I), which also absorbs light itself. LH-I then passes on the energy to a protein called the Reaction Center (RC), which is directly surrounded by LH-I forming the so-called LHI-RC complex. The RC, along with other proteins, then use this energy to facilitate a charge separation across the membrane. Finally, the potential gradient drives ATP synthesis by the ATP synthase protein. The entire process is summarized in Fig. 2.

While in most cellular processes, the proteins play the active role in the reactions, in photosynthesis, the protein components of LH-I, LH-II, and RC mostly exist as scaffolding to hold their cofactors in place. The primary pigments, bacteriochlorophylls (BChls) and carotenoids (Cars), are spread throughout both LH-I and LH-II, and few are also found in RC. These pigments are responsible for absorption of light energy, as well as the energy transfer to other pigments. By examining the LH proteins, one can look at how their sequences and structures determine how they arrange and bind to the pigments, and why the resulting pigment organization is well-suited for light absorption and excitation transfer, and therefore ideal for achieving high photosynthesis

efficiency. In this case study, we will investigate these concepts in the peripheral LH-II protein. This case study should take about three hours to complete.

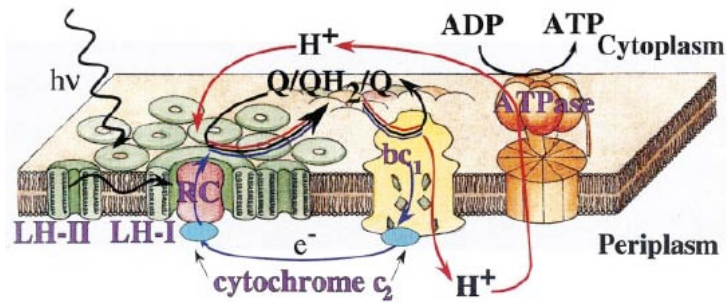


Figure 2: Schematic representation of the photosynthetic apparatus in purple bacteria intracytoplasmic membrane, adapted from [3]. Light is absorbed by the light harvesting complexes LH-I and LH-II, which pass their excitation energy to the reaction center (RC), where a charge separation is initiated. The charge gradient across the membrane then drives the ATPase to produce ATP, the energy form used by living organisms.

2 Structure of LH-II

In this section, we will start our investigation on LH-II protein by using VMD to explore its structure. We will mainly use the structurally available LH-II from a species of purple bacteria, *Rhodospseudomonas (Rps.) acidophila* [4], although LH-IIs from other species will also be discussed for comparison.

In all species of purple bacteria, LH-II forms a ring composed of identical units, with the number of units varying among species [5]. Each LH-II subunit consists of two transmembrane apoproteins, called the α - (inner) and β - (outer) apoproteins, and several pigment molecules, namely, carotenoids (Cars) and bacteriochlorophylls (BChls). In *Rps. acidophila*, the LH-II ring is composed of nine identical subunits, as shown in Fig. 3a.

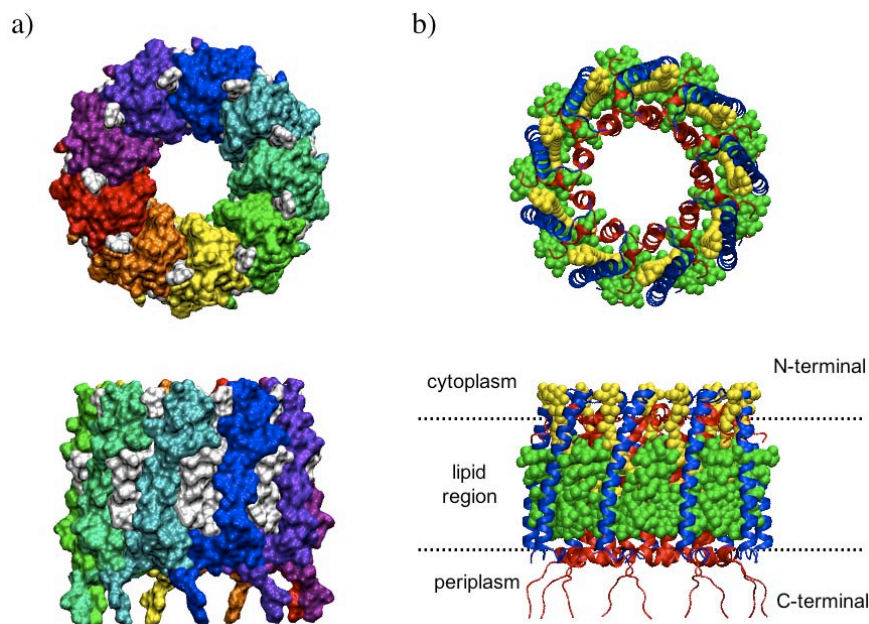


Figure 3: *Rps. acidophila* LH-II in two different representations. (a) Top view and side view of a full *Rps. acidophila* LH-II ring colored differently for each subunit and shown in surface representation in VMD. Pigments are colored white to be distinguished from the protein. In this representation one can see that *Rps. acidophila* LH-II is composed of nine identical subunits. (b) Top view and side view of *Rps. acidophila* LH-II in another representation. This time the protein is shown in New Cartoon to demonstrate its secondary structure. The α -apoproteins are colored red, while the β -apoproteins are colored blue. The BChls are shown in green and the Cars are shown in yellow in VDW representation. Dotted lines mark the approximate placement of lipid membrane around the LH-II.

2.1 Protein subunits

The protein component of each *Rps. acidophila* LH-II subunit consists of the α -apoprotein and the β -apoprotein, with the α -apoprotein forming the inner ring of radius 18 Å, and the β -apoprotein comprising the outer ring of radius 34 Å. The α - and β -apoproteins of *Rps. acidophila* contain 53 and 42 residues, respectively, with residues 12-35 in the α -apoprotein and 13-37 in the β -apoprotein making up the central hydrophobic region that is embedded in the lipid membrane. The N-terminal ends of both the α - and the β -apoprotein are on the cytoplasmic side of the membrane, while the

C-terminal sides are on the periplasmic side, as shown in Fig. 3b. The N-terminal and C-terminal regions of the α -apoproteins form small helices which lie in the plane of the membrane and “cap” the protein structure of the LH-II ring. The majority of the residues in the transmembrane region of both the α - and β -apoproteins are hydrophobic. However, some charged residues - histidines and arginines in particular - in the transmembrane region are important for pigment binding and interactions between adjacent protein subunits. The α and β -apoproteins are not connected to one another or to their neighbors in the ring, but are held together by van der Waals contact and hydrogen bonding with adjacent apoproteins and with the light-harvesting pigments, BChls and Cars in the complex.

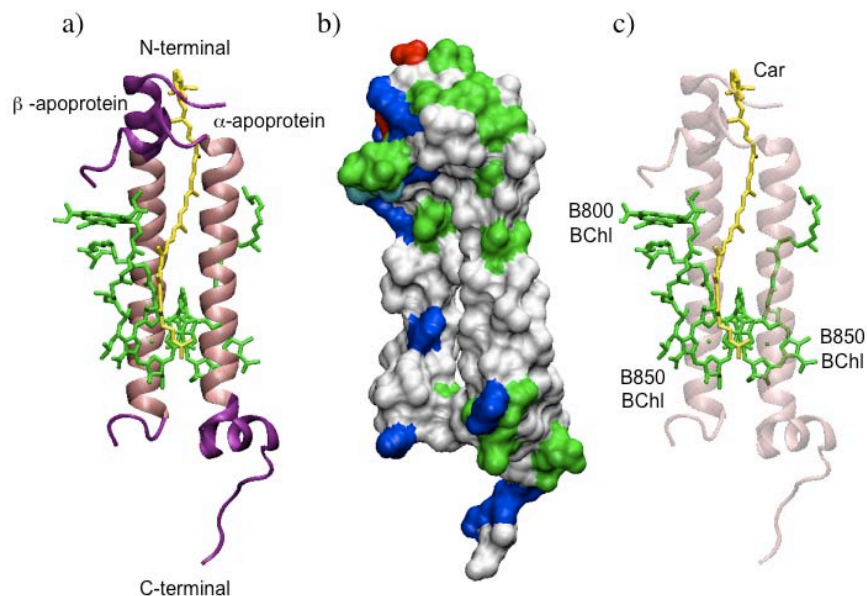


Figure 4: A single *Rps. acidophila* LH-II subunit in three different representations. Each LH-II subunit contains α - and β -apoproteins, three BChls and one Car. (a) The part of the apoproteins in lipid membrane is colored in pink, with the N- and C- terminal regions shown in purple. BChls are shown in green, while the Car is shown in yellow. (b) Transmembrane apoproteins shown in surface representation and colored by residue type: green is polar, white is hydrophobic, red is acidic (negatively charged), and blue is basic (positively charged). The majority of the residues which are in contact with the lipid membrane are hydrophobic. (c) Transmembrane apoproteins shown in transparent gray to highlight the positions of the pigments in the subunit.

2.2 Pigments

Besides the protein component, each LH-II subunit also contains three BChls and one Car [6]. The chemical structures of BChl and Car are shown in Fig. 5. There are several types of BChl; the one found in purple bacteria is called *bacteriochlorophyll a*, and it consists of a long hydrophobic phytol tail and a five-ring planar structure which has a magnesium atom at its center, as shown in Fig. 5a. Cars are long, hydrophobic molecules with a 40-carbon polyene chain and a head region that is unique to each variety. Different species of purple bacteria contain different types of Cars; for example, *Rps. acidophila* contains rhodopin glucoside, whereas *Rs. molischianum* contains lycopene and *Rb. sphaeroides* contains spheroidene (Fig. 5b).

Both pigments, BChls and Cars, form circular arrays in LH-II. The BChls form two separate

rings, one containing 18 BChls closer to the periplasmic side, and one containing 9 BChls closer to the cytoplasmic side. The BChls in the 18-fold ring are referred to as the B850 BChls, and those in the nine-fold ring are called the B800 BChls, after their respective absorbance wavelengths of 850 nm and 800 nm. We will explore the arrangement of the BChl molecules in greater detail in a later section. The Cars, which absorb at about 500 nm, wind between the α β -apoprotein pairs, providing structural support in addition to their role as pigments. In a later section, we will explore how these pigments are bound to the protein.

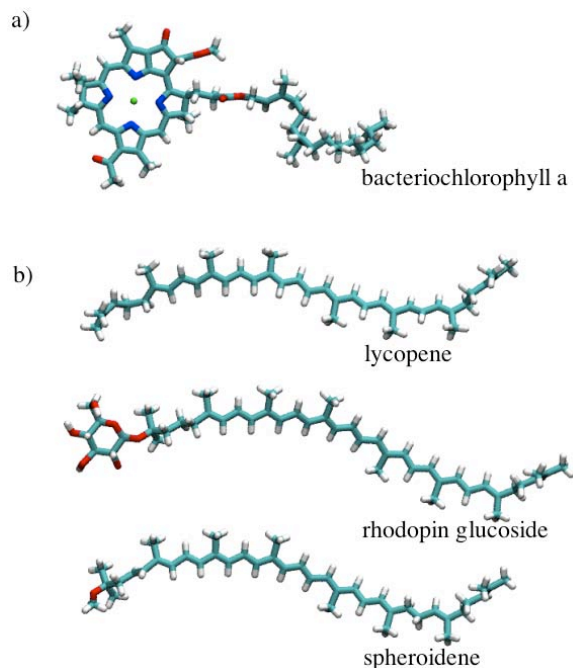


Figure 5: LH-II contains two types of pigments: (a) bacteriochlorophyll and (b) carotenoid. In this figure the molecules are colored by atom names: carbon in cyan, hydrogen in white, oxygen in red, nitrogen in blue, and magnesium in green. (a) *Bacteriochlorophyll a* is composed of a five-ring planar segment which binds a magnesium atom, and a long phytol tail. (b) There are many different types of carotenoids in different species or purple bacteria. Shown here are rhodopin glucoside, found in *Rps. acidophila*; lycopene, found in *Rs. molischianum*, and spheroidene, found in *Rb. sphaeroides*. All carotenoids contain a long carbon chain and differ only in their head region.

Exercise 1: General structural features of LH-II

In this exercise you will use VMD to verify the structural properties of *Rps. acidophila* LH-II described in this section. Load the provided coordinate file `acidophila-lh2.pdb` into VMD.

1. Create a representation with only the protein component of LH-II. You can do so by opening the Graphical Representations window via **Graphics** → **Representations** in the VMD Main window, and creating a new representation with “protein” being the Selected Atoms. Try using **Cartoon** or **New Cartoon** for Drawing Method. Can you see the double-ring structure of LH-II?
2. Hide all other representations and create a new representation for the BChls (**resname** `BCL` for Selected Atoms, **Licorice** for Drawing Method, and you can choose any Coloring Method). Continue with the previous representation but change the Selected Atoms to **resname** `RG1` to show all the Cars. Can you see the rings formed by the pigment molecules?
3. Try to reproduce the top view of LH-II in Fig. 3b, and save an image of your view via **File** → **Render...** on the VMD main menu.
4. Hide any representation with pigments, show only the representation with the protein component of LH-II, and color it by **ResType**. Where are most of the charged residues located? Closer to the cytoplasmic side or the periplasmic side? Where are the hydrophobic residues located, in relation to where the protein would sit in the lipid membrane?
5. Create another representation for the histidine residues (**resname** `HIS` for Selected Atoms and **VDW** for Drawing Method, choose any coloring method that makes it easier for you to identify them). How many histidine residues are found in each α -apoprotein? How many histidine residues are found in each β -apoprotein? What are their residue numbers?

2.3 Comparison of LH-II from different species of purple bacteria

Rps. rubrum and *Rps. viridis* are the only species of purple bacteria without LH-II. All other species have LH-IIs that are very similar structurally to the LH-II of *Rps. acidophila*. Currently, high-resolution structures exist for only two species of purple bacteria - *Rps. acidophila* [4] and *Rs. molischianum* [7]. In this section, we will compare the structures of the LH-IIs from these two species.

Like *Rps. acidophila*, *Rs. molischianum* LH-II is a ring composed of identical subunits, each containing two B850 BChls, one B800 BChl, as well as one carotenoid which, in its case, is lycopenene. It also contains transmembrane α - and β -apoproteins which are similar to those found in *Rps. acidophila* LH-II, both in structure and in sequence. However, *Rs. molischianum* LH-II contains only eight subunits where *Rps. acidophila* contains nine. Although it is not known why each species adopts a different oligomerization, this topic has been explored via molecular dynamics simulations which suggest that surface contacts in the transmembrane region drive a preferred angle at which the two LH-II subunits aggregate: 42.5 degrees for *Rs. molischianum* and 38.5 degrees for *Rps. acidophila* [8]. This difference in aggregation angle may cause the difference in the preferred oligomerization between the two species. A coordinate file of the *Rs. molischianum* LH-II

is provided as `molischianum-lh2.pdb`, which you may load into VMD to explore these features.

Now we will explore the similarities between the two LH-II subunits in more detail by doing a structural alignment using the VMD plugin MultiSeq (which you will reproduce in Exercise 2). A structural alignment finds the best alignment for two similar structures by finding their relative orientation with the minimal RMSD. Proteins that perform similar functions often display structural similarities. Since the function of the two LH-II complexes is the same - to provide a scaffold for the light-harvesting pigments - one would expect to see a high degree of structural similarity between them.

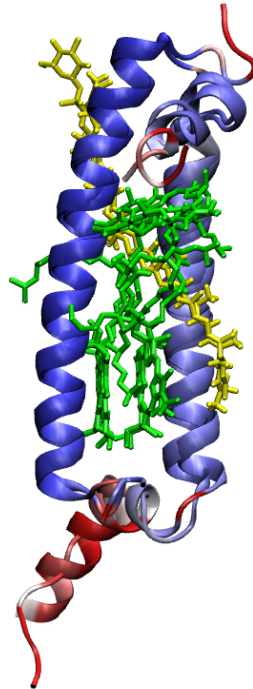


Figure 6: Structural alignment of *Rps. acidophila* and *Rs. molischianum* LH-II subunits and bound pigments. The proteins are colored by Qres, which measures how well two structures fit. A higher value of Qres (colored blue) indicates a higher degree of structural similarity, while a lower value of Qres (colored red) indicates less similarity between the aligned structures. Note the excellent alignment of the transmembrane helices and pigments.

Exercise 2: Structural alignment of LH-II subunits

In this exercise, you will produce a structural alignment between the LH-II subunits of *Rps. acidophila* and *Rs. molischianum*. Load `molischianum-unit.pdb` and `acidophila-unit.pdb` into VMD. Go to the Graphical Representations window and create the following representations:

for `acidophila-unit.pdb`:

- a. Selected Atoms: `protein`, Drawing Method: `NewCartoon`
- b. Selected Atoms: `resname BCL RG1`, Drawing Method: `Licorice`

for `molischianum-unit.pdb`:

- a. Selected Atoms: `protein`, Drawing Method: `NewCartoon`
- b. Selected Atoms: `resname BCL LYC`, Drawing Method: `Licorice`

From the VMD Main window, open MultiSeq via `Extensions` → `Analysis` → `MultiSeq`. Select `acidophila-unit_A` (the α -apoprotein of *Rps. acidophila*) and `molischianum-unit_A` (the α -apoprotein of *Rs. molischianum*) by checking their selection boxes, and go to `Tools` → `Stamp Structural Alignment`. Choose the `Marked Structures` option, leave everything else unchanged, and click OK. MultiSeq will now align these two selections so that they are as well fitted structurally as possible.

We also want to align the β -apoproteins by unchecking `acidophila-unit_A` and `molischianum-unit_A`, and selecting `acidophila-unit_B` and `molischianum-unit_B`. Repeat the steps to align the β -apoproteins. Now on your VMD OpenGL Display, the LH-II subunits should be aligned and overlapping.

If you hide all other representations and keep only the protein representations, you can see that the LH-II subunits fit very well on top of each other. But we would like a measure of how well the alignment is and how much are the two subunits structurally similar. This measure is the Qres value, and MultiSeq allows one to color the alignment by their Qres. In the MultiSeq window, make sure you only check `acidophila-unit_A` and `molischianum-unit_A`, go to `View` → `Coloring`, make sure the `Apply to Marked` box is checked, and select `Qres` to color the α -apoproteins by Qres. Do the same for the β -apoproteins by unchecking `acidophila-unit_A` and `molischianum-unit_A` and checking `acidophila-unit_B` and `molischianum-unit_B`, and repeating the steps. Now in your VMD OpenGL window the subunits are colored by their Qres values. A higher value of Qres (colored blue) indicates a higher degree of similarity, while a lower value of Qres (colored red) indicates less similarity between the aligned structures.

The result of the alignment is shown in Fig. 6. You can see that the transmembrane helices of both species align very well with one another. The only part of the proteins that do not align well are the inward-bent helical “caps” at the N-terminus. Although each species contains a different kind of carotenoid, both are in the same place between the α - and β -apoproteins, as are the BChls of both species. This seems to imply that the pigment molecules are bound in each species in approximately the same way.

Save an image of your alignment via `File` → `Render...` in VMD.

3 Alignment of Multiple LH-II Sequences

The structure of a protein strongly depends on its amino acid sequence, and the structural features of a protein are closely related to its functional properties. This “sequence→structure→function” relationship in proteins implies that understanding the function of a protein requires understandings of both its structure and sequence. In the previous section, we looked at general structural features of LH-II, and in this section, we will discuss the sequence of LH-II, in particular, the sequences of the α - and β -apoproteins.

Since a protein’s sequence is related to its function, one would expect that two proteins serving an identical purpose should exhibit great sequence similarity. In this section, we will show that the sequences of α - and β -apoproteins of LH-II from different species of purple bacteria share many common features. To compare these sequence, we will apply a very useful plugin of VMD, the MultiSeq plugin¹.

The process of comparing sequences is called sequence alignment. This is a particularly useful method for recognizing what part of an amino acid chain is responsible for a particular protein function. It is also a useful method for protein structure prediction when a protein’s structure is unknown but the structure of a protein with the same function is available. The sequence alignment will be done in Exercise 3, with a suggestive result given in Fig. 7.

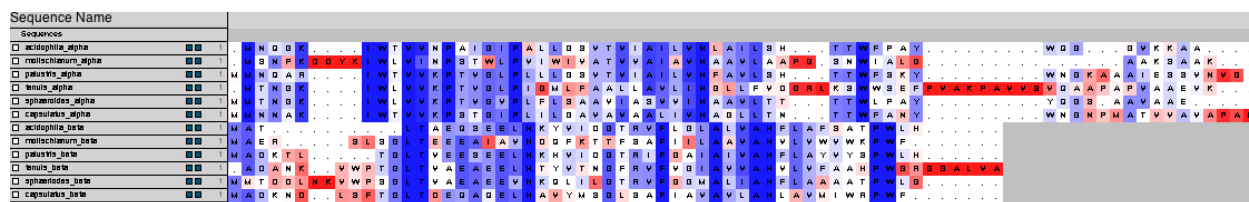


Figure 7: Multiple sequence alignment of LH-II α - and β -apoproteins from six species of purple bacteria (*Rps. acidophila*, *Rps. molischianum*, *Rps. palustris*, *Rb. sphaeroides*, *Rb. capsulatus*, and *Rc. tenuis*). The sequences are colored according to sequence similarity, where blue means more similar and red means less similar. You can see that the sequences are quite similar overall.

¹For more information on the plugin, including a tutorial and the MultiSeq paper [9], one can consult <https://www.ks.uiuc.edu/Research/vmd/plugins/multiseq>.

Exercise 3: Sequence alignment of LH-II α - and β -apoproteins

In this exercise, you will produce sequence alignments for the α - and β -apoproteins from six different species of purple bacteria: *Rps. acidophila*, *Rs. molischianum*, *Rps. palustris*, *Rb. sphaeroides*, *Rb. capsulatus*, and *Rc. tenuis*. Two fasta files have been provided for this exercise: `alpha.fasta` and `beta.fasta`. A fasta file stores a protein's sequence information in plain text as a sequence of the one-letter amino acid codes. You can open the fasta files with a text editor to view their contents. `alpha.fasta` and `beta.fasta` contain the amino acid sequences of the α - and β -apoproteins from the six species of purple bacteria.

We will start by aligning the sequences of LH-II α -apoproteins by following the steps:

1. In a new VMD session, open MultiSeq via **Extensions** \rightarrow **Analysis** \rightarrow **MultiSeq**. In the MultiSeq window, go to **File** \rightarrow **Import Data**, and use the top Browse button to load the file `alpha.fasta`.
2. Align all the sequences of the α -apoproteins via **Tools** \rightarrow **ClustalW Sequence Alignment**, leave all options unchanged, and click OK. You should see some change in your MultiSeq window as the sequences now have been aligned.
3. Color the sequences by sequence similarity: go to **View** \rightarrow **Coloring** \rightarrow **Sequence Similarity** \rightarrow **BLOSUM70**. The aligned sequences are now colored by sequence similarity; blue denotes residues that are highly conserved among sequences from different species, whereas red denotes residues that are poorly conserved. Your MultiSeq window should resemble Fig. 7.

1. Which residues in LH-II α -apoproteins are conserved among all species? You will see why some of these conserved residues are significant in the next section. By highlighting any two sequences by Ctrl-clicking in the MultiSeq window, you can also see what percentage of residues are conserved between any two sequences. What percentage of residues are conserved between the α -apoproteins of *Rps. acidophila* and *Rs. molischianum*?

2. Do a sequence alignment for the LH-II β -apoproteins by loading `beta.fasta` into MultiSeq and repeating the steps above (it might be a good idea to start a new VMD session). Which residues are conserved in the β -apoproteins of all species? What percentage of residues are conserved between the β -apoproteins of *Rps. acidophila* and *Rs. molischianum*?

4 Chlorophyll Binding Sites

In a way, the protein components of the LH-II complex exist merely as a scaffold for the light-absorbing pigment molecules, ensuring that the positions and orientations of the BChls and Cars are optimal for light-absorption and energy transfer. In another way, the presence of the pigments and their binding with the protein stabilize the overall structure of the LH-II ring. Either way you look at it, the binding between the pigments and the protein is essential for LH-II structural integrity as well as its function. In this section we will look at how pigments BChls and Cars bind to the LH-II protein.

In Exercise 3, you should have noticed that two histidine residues, one in the α -apoprotein and one in the β -apoprotein, are highly conserved among all purple bacteria LH-II. This is not a coincidence, as these two histidine residues serve an important function that's necessary in all LH-II: they provide the binding sites for the B850 BChls. As shown in Fig. 8a, in each LH-II subunit, the magnesium atoms of the two B850 BChls each binds to a nitrogen atom of a histidine, one in the α -apoprotein and one in the β -apoprotein.

The B800 BChls are ligated in a different way - the first residue of the α -apoprotein in *Rps. acidophila*, a carboxylated methionine, ligates to the central magnesium of B800 BChl [4] (Fig. 8b). For *Rs. molischianum*, the first residue of its LH-II α -apoprotein is not methionine but aspartic acid, however it binds to the corresponding B800 in an analogous way.

In addition to these ligation sites, the BChls are further stabilized by hydrogen bonds and van der Waals contact with the protein and with other BChls. The rings of the B850 BChls hydrogen bond to α -Trp45 and α -Tyr44, and the B800 BChl hydrogen bonds to β -Arg20; in addition their phytol tails are in close contact with many residues in the protein scaffold. The phytol tail of the β -bound B850 also wraps around the phytol tail of the B800 and makes van der Waals contact with the face of the B800.

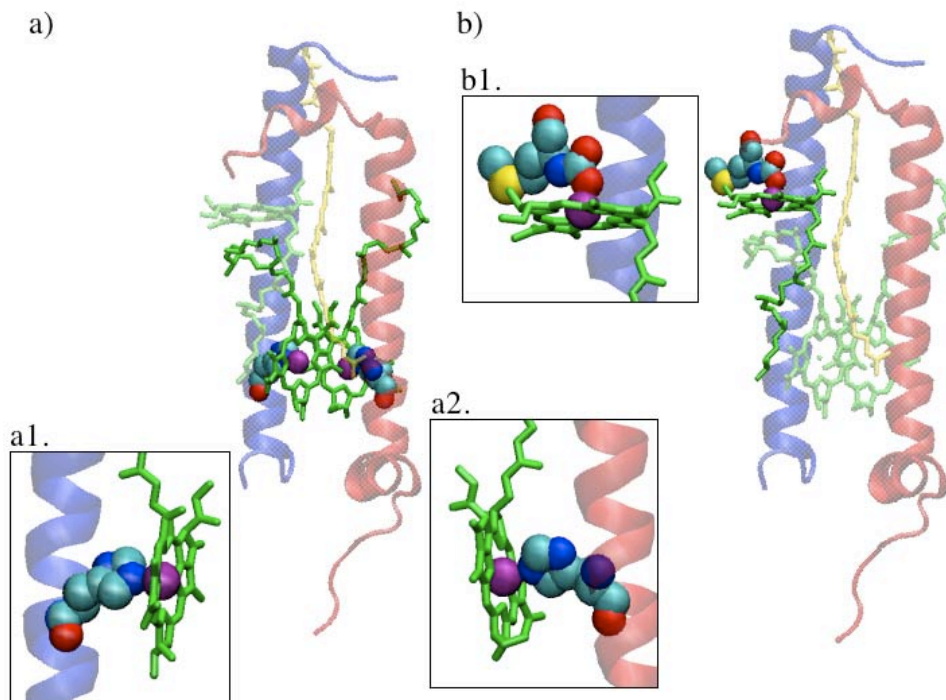


Figure 8: (a) The B850 BChls are liganded to the α - and β -apoproteins via two highly conserved histidine residues: HIS31 in the α -apoprotein and HIS30 in the β -apoprotein. These histidines bind to the magnesium atoms of B850 BChls. (b) In *Rps. acidophila* LH-II, the B800 BChl is held in place by the N-terminal carboxylated methionine of the α -apoprotein.

Exercise 4: B850 binding sites

Load `acidophila-unit.pdb` into VMD, and create the following representations:

- Selected Atoms: `protein`, Drawing Method: `NewCartoon`, Coloring Method: `ColorID - 8 white`
- Selected Atoms: `resname BCL` and `resid 301 302`, Drawing Method: `Licorice`, Coloring Method: `ColorID - 7 green`
- Selected Atoms: `name MG` and `resid 301 302`, Drawing Method: `VDW`, Coloring Method: `ColorID - 11 purple`
- Selected Atoms: `chain A` and `resid 31`, Drawing Method: `CPK`, Coloring Method: `Name`
- Selected Atoms: `chain B` and `resid 30`, Drawing Method: `CPK`, Coloring Method: `Name`

These selections are for *a.* the α - and β -apoproteins, *b.* the two B850 BChls, *c.* the magnesium atoms for the two B850 BChls, *d.* the histidine residue in the α -apoprotein that binds to one of the B850 BChls, and *e.* the histidine residue in the β -apoprotein that binds to the other B850 BChl.

- Measure the distances between the magnesium atoms in the BChls and the binding nitrogen atoms in the liganding histidines (click `Mouse` \rightarrow `Label` \rightarrow `Bonds` from the VMD Main window to measure the distance between two atoms).
- Histidines have two possible protonation states: HSE, where the proton resides on the epsilon nitrogen (`name: NE2`), and HSD, where the proton resides on the delta nitrogen (`name: ND1`). Should the liganding histidines in the α - and β -apoproteins be HSE or HSD type? Why? Hint: Use VMD to look at which nitrogen of the histidine ligands to the magnesium atoms of B850 BChls - is it possible for another hydrogen atom to bind to this nitrogen?

5 Pigment Organization

As seen from previous sections of this case study, LH-II contains two types of pigments: carotenoids (Cars) and bacteriochlorophylls (BChls). We have also been introduced to their general placements in the protein. In this section we will further explore the intricate organization of the pigments, and prepare ourselves for the discussion of how collective geometrical features, such as pigment molecules' relative orientation and their distances, facilitate the process of excitation transfer among different pigments.

5.1 The BChl rings

One of the most interesting features of purple bacteria LH-II is the organization of circular BChl aggregates. As seen from Section 2, the BChls in *Rps. acidophila* LH-II form two rings. The ring closer to the cytoplasmic side is more loosely packed, and it consists of nine B800 BChls. Each B800 BChl is ~ 21 Å from its nearest neighboring B800 BChls (Mg-Mg distance), as seen in Fig. 9a.

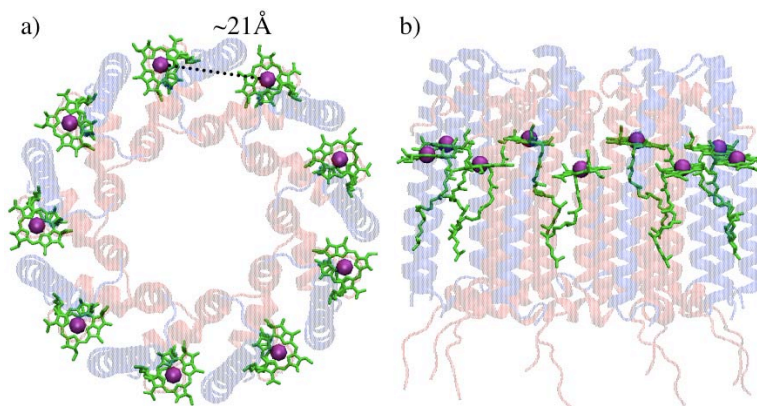


Figure 9: VMD images of the *Rps. acidophila* B800 BChl ring, a) top view and b) side view. The B800 BChls are drawn in `Licorice` representation and colored in green, and the magnesium atoms shown in `VMD` representation and colored in purple. The proteins are drawn in `New Cartoon` representation, with the α -apoproteins colored in transparent red and the β -apoproteins in transparent blue. One can measure the nearest neighbor Mg-Mg distance with VMD and obtain a ~ 21 Å separation. Not shown here are the B850 BChls and the Cars. You will replicate this representation with the B850 BChl ring in Exercise 4.

Closer to the periplasmic side of LH-II lies another bacteriochlorophyll ring. This more tightly packed ring has eighteen B850 molecules. At first look one might think the distance between any two nearest neighbor B850 molecules is the same. But by measuring all nearest neighbor distances with VMD (Exercise 4), one finds that the B850 ring is actually a dimerized aggregate, with alternating nearest neighbor Mg-Mg distances along the ring.

Exercise 5: The dimerized B850 ring

1. Open a new VMD session and load the pdb file `acidophila-lh2.pdb`. Make a representation that shows only the B850 ring, much like Fig. 9, but with only the eighteen B850 BChls. Note the B850 ring can be specified by the selection `resid 301 to 306`. Save your VMD image, either by taking a snap shot of your computer screen, or by using the image rendering feature of VMD via `File` → `Render...` on the VMD main menu.

2. Measure all eighteen nearest neighbor Mg-Mg distances of the B850 ring by using the `Mouse` → `Label` → `Bonds` function in VMD, and write the distances down. Do you see a pattern? (Hint: Your answer should alternate between ~ 9.5 Å and ~ 9 Å. Also, since this coordinate file was actually built by replicating three LH-II subunits into nine subunits, you will see a repetition pattern.)

Keep this VMD session open, you will come back to it later.

5.2 Carotenoid ring

In purple bacteria LH-II, not only do the BChls form circular aggregates, the other type of pigment, the Cars, also have this similar organizational property. In *Rps. acidophila* LH-II, nine carotenoids form a ring in the space between the α - and β -apoproteins, as shown in Fig. 10. The long carotenoid molecules effectively “bolt” the adjacent $\alpha\beta$ -apoprotein pairs together, thus adding stability to the LH-II structure. Besides this structural role, carotenoids also have other two very important functions. First, since carotenoids absorb at a different energy level than BChls, they thereby act as accessory LH-II pigments and allow LH-II to harvest light at a wider spectral range. Second, and perhaps the most important contribution of carotenoids, is that they prevent the formation of very fatal singlet oxygen molecules that can destroy a cell. We will discuss this feature in greater detail in the next section.

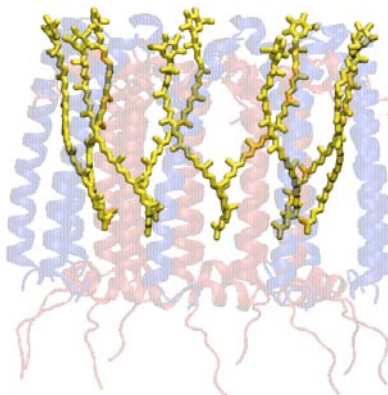


Figure 10: A VMD image of the carotenoid ring in acidophila LH-II. The carotenoid molecules are shown in Licorice representation and colored yellow, with the rest of the protein outlined by the New Cartoon representation in transparent red and blue.

Due to their long molecular structures, carotenoids span from the periplasmic side to the cytoplasmic side of LH-II, and are hence in close contact with both the B800 and B850 BChls (Fig. 11).

Such proximity allows carotenoids to interact with both types of BChls via electron exchange mechanism, which we will discuss in the following section.

Exercise 6: Measuring the distances between Car and B800/B850 BChls

Return to your VMD session, hide or delete all previous representations. 1. Try to replicate the VMD image in Fig. 11 by making the following selections and representations:

- display one of the nine carotenoids by making the selection “resname RG1 and resid 403 and segname A”
- display the closest B800 bacteriochlorophyll from the carotenoid selected in *a.* by making the selection “resname BCL and resid 308 and segname A”
- display the closest B850 bacteriochlorophyll from the carotenoid selected in *a.* by making the selection “resname BCL and resid 301 and segname B”

2. Measure the closest distance between the Car and B800 BChl in VMD, as marked by the black dotted line in Fig. 11.

3. Measure the closest distance between the Car and B850 BChl in VMD, as marked by the black dotted line in Fig. 11.

Keep this VMD session open, as you will continue using it for the next few exercises.

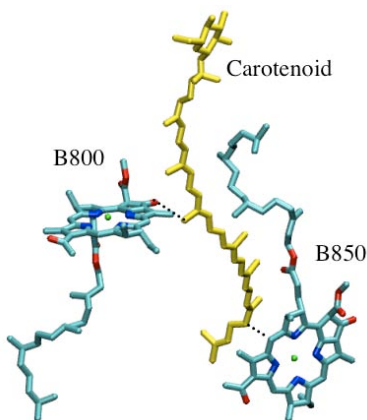


Figure 11: VMD image of one carotenoid molecule next to its closest B800 and B850 BChls, with the dotted lines indicating the closest distances. All molecules are drawn in Licorice representation.

5.3 Circular aggregates and symmetry of LH-II pigments

In *Rps. acidophila* LH-II, pigments form circular aggregates with apparent symmetry properties. The nine B800 BChls form a ring with nearest neighbor Mg-Mg distance of ~ 21 Å. The eighteen B850 BChls form a dimerized ring with alternating nearest neighbor Mg-Mg distance of less than 10 Å, as seen in Exercise 4. The Cars also form a ring, and are within few Ås of both the B850 and B800 BChls.

Such highly symmetric pigment organization is observed in the light harvesting complexes of other photosynthetic bacteria as well. For example, the purple bacterium *Rs. molischanum* LH-II also has a B850 ring, a B800 ring, and a Car ring, all with similar geometrical properties as the circular pigment aggregates in *Rps. acidophila* LH-II. For higher organisms like plants and cyanobacteria, however, the pigment organizations exhibit no such apparent symmetry, as shown in Fig. 12. Although the pigments in plants and cyanobacteria are arranged in a seemingly random array, the excitation transfer process among the pigments in these organisms is no less efficient than that carried out in purple bacteria. It is hence an interesting question why higher organisms have chosen a less symmetrical pigment array for photosynthetic apparatus through evolution. The discussion on the evolutionary process of photosynthetic apparatus is out of the scope of this case study, but one can consult [10, 11] for studies on this topic.

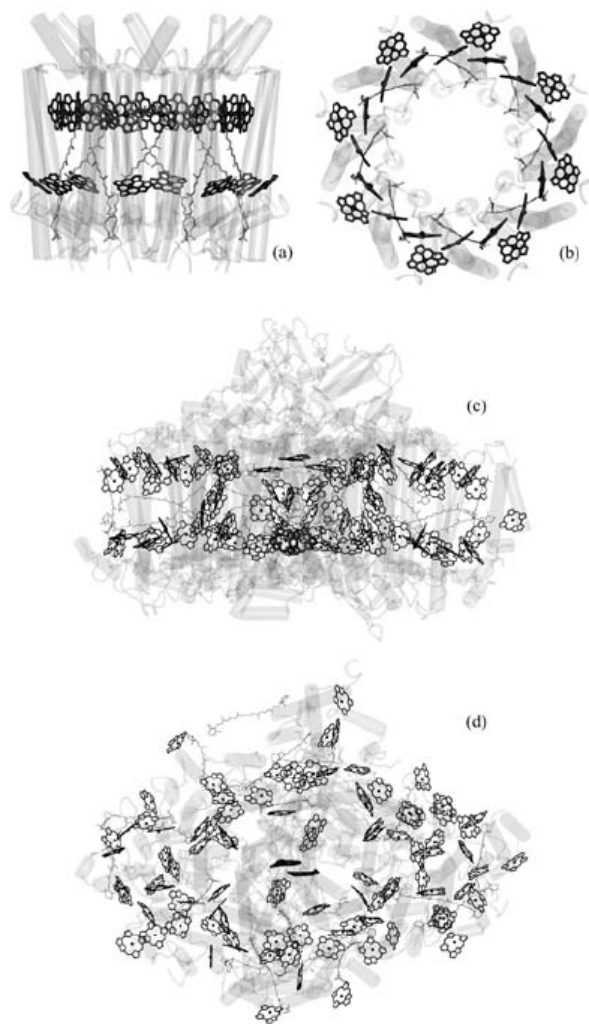


Figure 12: Comparison of pigment organizations in purple bacteria and cyanobacteria, adapted from [12]. BChls are shown in black, and for simplicity only the bacteriochlorin ring is shown. The carotenoids are shown in gray. The proteins are drawn in transparent grayscale. (a) Side view of the symmetrical pigment organization in purple bacterium *Rs. molischianum* LH-II. The BChls form two rings and the Cars form another one. (b) Top view of *Rs. molischianum*. (c) Side view of the pigments in cyanobacterium *Synechococcus elongatus* light harvesting complex photosystem I. The pigments in *Synechococcus elongatus* photosystem I show no apparent symmetry. (d) Top view of *Synechococcus elongatus*.

6 Excitation Transfer in LH-II

After light is absorbed by pigments in LH-II, the pigments need to transport their excitation energy to LH-I and eventually to the reaction center where the photosynthetic process is facilitated. In this section we will study the excitation transfer process among different pigments in LH-II. We will see that all organizational features of the pigments we have seen so far determine which methods one chooses to better describe the various excitation transfer processes that occur in LH-II among different pigments.

6.1 Introduction to excitation transfer

The process of electronic excitation transfer between two spatially separated molecules D (donor) and A (acceptor) can be represented by the following scheme



Eqn. 1 describes the process in which donor molecule D transfers its excitation (denoted by $*$) to acceptor molecule A . Initially, molecule D is in its excited state D^* and molecule A is in its ground state. After the excitation transfer reaction, D is deexcited to its ground state and its energy moves A to its excited state A^* . As presented in Fig. 13, there are two possible mechanisms for such excitation transfer to occur: Coulomb mechanism is effective over molecule distances of typically 20-50 Å, while for molecules within few Ås the electron exchange mechanism is used [13].

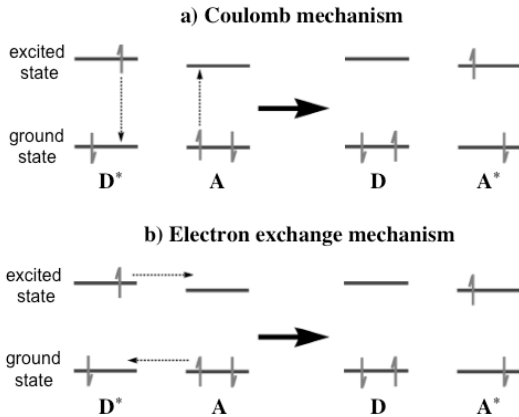


Figure 13: Two mechanisms of excitation transfer, (a) Coulomb mechanism, and (b) electron exchange mechanism. In Coulomb mechanism, the energy is transferred from the donor to the acceptor molecules via electronic coupling, and better describes the excitation transfer between molecules separated by $\sim 20\text{-}50$ Å. In the electron exchange mechanism, which requires close contact between the donor and the acceptor molecules, the excited electron in the donor molecule is exchanged with a ground state electron in the acceptor molecule to complete the excitation transfer process. Figure is adapted from [14].

Typically, excitation is transferred from a molecule at a higher energy level to a molecule at a lower energy level; hence, one can speculate the possible excitation transfer paths in LH-II by looking at the pigments' energy levels. As shown in Fig. 14, Car has two excitation states that are known to be involved in the LH-II excitation transfer process, namely, the S_1 and S_2 states. When a Car absorbs light, it is excited to its second excited state, S_2 , and can then either relax to

its lower excited state, S_1 , or give its excitation energy to B800 or B850 BChls, which both have excitation states with lower energies than S_2 .

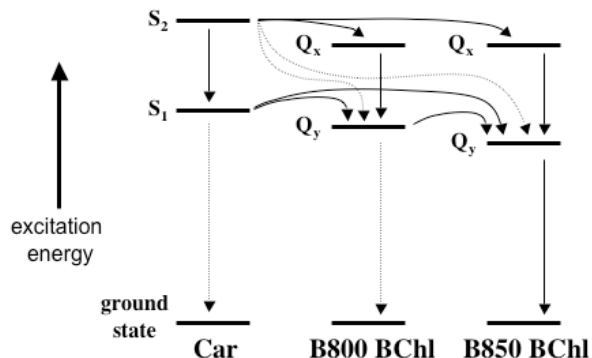


Figure 14: Energy levels of the electronic excitation of BChls and Cars and their possible excitation transfer paths, adapted from [13, 15]. The Cars have two known excitation states that are involved in the electron transfer process, namely, first excitation state S_1 and second excitation state S_2 . The BChls have two main excitation states, first excitation state Q_y and second excitation state Q_x . The arrows indicate possible excitation transfer paths among different pigments, with solid arrows representing major excitation transfer paths, and dashed arrows representing minor or speculated transfer paths.

For the BChls, absorbing a photon pumps them to their lowest excitation state, the so-called Q_y state, which is associated with a dipole moment connecting the B and D nitrogens (Fig. 15). The second excitation state is the Q_x state, associated with a dipole moment connecting the A and C nitrogens (Fig. 15). The excitation states of B800 BChl are lower than the excitation states of B850 BChl, making it possible for B800 BChls to transfer their excitation energy to B850 BChls.

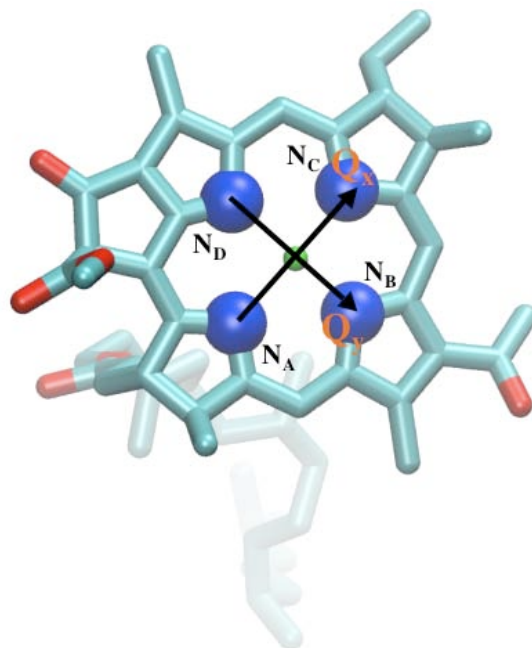


Figure 15: Excitation dipole moments of BChl. The dipole moment associated with the first excitation state, Q_y , has a direction along the line connecting the B and D nitrogens. The dipole moment associated with the second excitation state, Q_x , has a direction along the line connecting the A and C nitrogen.

Exercise 7: Dipole moments of BChl excitation states

1. Return to the VMD session that you have created for the previous two exercises. Hide or delete all previous representations. Create a new representation for `resname BCL and resid 301 and segname A`, which gives you a single B850 BChl. Identify the B and D nitrogen atoms for this B850 BChl, and described the direction of its Q_y dipole moment. In particular, is this vector approximately parallel or perpendicular to the plane of the membrane? (Hint: The B and D nitrogen atoms are specified by `name:NB` and `name:ND`).

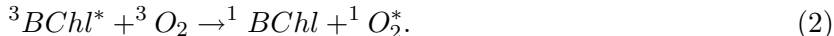
2. Hide the B850 BChl representation and create a new representation for a single B800 BChl by selecting `resname BCL and resid 308 and segname A`. Again identify its B and D nitrogen atoms and described the direction of its Q_y dipole moment. In particular, is this vector approximately parallel or perpendicular to the plane of the membrane?

The answers you got from the previous two questions should tell you that B850 and B800 BChls have approximately perpendicular Q_y dipole moments. Similarly, their Q_x dipole moments are also perpendicular (feel free to check with VMD!). This result, which stems from the geometrical placement of the BChls, suggests that the relative orientation of the B850 and B800 rings actually has an important functional feature, namely, it allows LH-II to absorb light coming from different directions!

Again, keep this VMD session.

6.2 Car \leftrightarrow BChl excitation transfer

Having introduced the basics of the excitation transfer process, let's start our discussion of the various excitation transfer channels in LH-II. From Fig. 14, we see that Car absorbs light and transfers its energy to BChls, and hence, as mentioned before, allows LH-II to harvest a wider spectral range of light. But BChls actually also pass their excitation to Car for another important function. Without Car, excited BChl triplets can collide and react with triplet oxygens to produce harmful singlet oxygens according to the following chemical reaction:



The singlet oxygen, ${}^1\text{O}_2^*$, produced in Eqn. 2 is a very dangerous oxidizing agent. It oxidizes nearby conjugated double bonds and leads to cell death. Car prevents the harmful reaction in Eqn. 2 by interacting itself with the excited BChl triplet in the following way:



The reaction in Eqn. 3 occurs at a faster time scale than the reaction in Eqn. 2, hence, the existence of Car effectively prevents the production of lethal singlet oxygens and avoids cell death.

In Exercise 4 we have seen that Car is only few Ås from its nearest B800 and B850 BChls. This close proximity puts Car in van der Waals contact with both B800 and B850 BChls, making electron exchange mechanism the more likely excitation transfer process that occurs between Car and BChls. In fact, it is known that the triplet-triplet BChl \rightarrow Car energy transfer described in Eqn. 3 takes place via an electron exchange mechanism [16]. However, the photochemistry in the Car \rightarrow BChl excitation transfer process is more complicated. As shown in Fig. 14, there are four major transfer channels from Car to BChls: Car S_2 state \rightarrow B800 Q_x state, Car S_2 state \rightarrow B850 Q_x , Car S_1 state \rightarrow B800 Q_y state state, and Car S_1 state \rightarrow B850 Q_y state. Each of these four paths is best described by different excitation transfer mechanisms and has different efficiency and time scale that's highly dependent on the transition dipole geometries of the excitation states and the molecules' internal symmetry. Furthermore, it is speculated that Car has more excitation states in addition to S_1 and S_2 that also participate in the Car \rightarrow BChl excitation transfer process. The topic on the theoretical description of Car \rightarrow BChl excitation transfer is interesting but also well beyond the scope of this case study. We will hence not dwell upon further details, but point out that, if the excitation transfer only takes place from S_2 , then the overall Car \rightarrow BChl efficiency is limited to $\sim 50\text{-}60\%$, but if S_1 also participates in the Car \rightarrow BChl excitation transfer, then the efficiency is calculated to reach nearly 100% [5].

6.3 B800 \leftrightarrow B800 excitation transfer

B800 BChls can be excited either by absorbing light or by receiving excitation energy from Car. The excitation energy of B800 BChls can be transferred to B850 BChls, or can also "hop around" in the B800 BChl ring (*i.e.* the B800 \leftrightarrow B800 excitation transfer). As seen in Exercise 4, each B800 is at least 20 Å from its closest neighbor, making Coulomb mechanism the more accurate description for the excitation transfer that takes place within the B800 ring. In particular, given that the excitation states of BChls are characterized by representative dipole moments, one can approximate the interaction energy H_{ij} between any two B800 BChls i and j with the Coulomb coupling

$$H_{ij} = C \left[\frac{\vec{d}_i \cdot \vec{d}_j}{r_{ij}^3} - \frac{3(\vec{r}_{ij} \cdot \vec{d}_i)(\vec{r}_{ij} \cdot \vec{d}_j)}{r_{ij}^5} \right], \quad (4)$$

where \vec{d}_i is the unit vector along the direction of the i -th BChl's dipole moment, \vec{r}_{ij} is the vector connecting the magnesium atoms of the i -th and j -th B800 BChls, and C is the coupling constant. Conventionally the interaction energy H_{ij} is expressed in terms of wavenumbers cm^{-1} , with the conversion relation $1 \text{ cm}^{-1} = 1.986 \times 10^{-23}$ Joules. The coupling constant C for *Rps. acidophila* B800 BChls is $C = 189513.5 \text{ \AA}^3 \text{ cm}^{-1}$ [5].

Exercise 8: Coupling Energy of B800

In this exercise, we will use Eqn. 4 to compute the coupling energy between a pair of B800 BChls.

1. Go back to the VMD session you have created. Hide all representations from previous exercises, and create a new representation for a pair of nearest-neighbor B800 BChls. You can choose any nearest neighbor pair among the nine B800 BChls. Write down the representation(s) you have used to select these B800 BChls.

2. To use Eqn. 4, we need to first measure the following quantities with VMD: \vec{d}_i , \vec{d}_j , and \vec{r}_{ij} . For one of the B800 BChls, calculate its dipole moment vector by measuring the position of the B and D nitrogens. Don't forget to normalize the dipole vector for \vec{d}_i .

3. Similarly, measure \vec{d}_j for the other B800 BChl.

4. Compute \vec{r}_{ij} by measuring the positions of the two Mg atoms in both B800 BChls. You should also measure the Mg-Mg distance r_{ij} .

5. Plug in all the quantities you have collected into Eqn. 4, and compute the interaction energy H_{ij} . Your answer should be somewhere around -24 cm^{-1} , as computed in [5].

Hint: If you get lost in the calculation and cannot get the final answer of $\sim -24 \text{ cm}^{-1}$, try all the questions again with this pair of nearest-neighbor B800: **resid 307 and chain X and segname B** and **resid 309 and chain X and segname A**. For this pair of B800 the \vec{d}_i and \vec{d}_j would be (0.154, 1.000, -0.152) and (0.754, -0.643, -0.131), the \vec{r}_{ij} would be (-17.888, -11.441, 0.069), which gives $r_{ij} = 21.234$. With these parameters, Eqn. 4 gives $\sim -21.5 \text{ cm}^{-1}$.

You may now finally end this VMD session. We will no longer require its service.

We have seen that by applying Eqn. 4 and using VMD to measure relevant coordinate information, one can obtain the interaction energy H_{ij} between any two B800 BChls. In Exercise 7 we measured H_{ij} for a pair of nearest neighbor B800 BChls. One can use the exact same procedure to measure H_{ij} between a pair of non-nearest neighbor B800 BChls, but since H_{ij} is proportional to $1/r_{ij}^3$, H_{ij} decreases very quickly over longer BChl-BChl distances.

The interaction energy H_{ij} then allows one to compute the rate of excitation transfer between any pair of B800 BChls via the equation

$$T_{ij} = \frac{2\pi}{\hbar} |H_{ij}|^2 \int S_i^D(E) S_j^A(E) dE, \quad (5)$$

where $S_i^D(E)$ and $S_j^A(E)$ are the emission spectrum of pigment i and the absorption spectrum for pigment j , respectively. Hence the integral $\int S_i^D(E) S_j^A(E) dE$ measures the spectral overlap between pigments i and j . One can then compute the rate of excitation transfer given the spectral information on the BChl pigments. The B800-B800 excitation transfer timescale has been experimentally measured to be around 1.5 ps [5].

6.4 B800 \rightarrow B850 excitation transfer

The singlet-singlet excitation transfer from B800 to B850 is perhaps one of the most extensively studied kinetic processes in bacterial light harvesting [15]. Early time-resolved experiments have estimated the time scale for B800 \rightarrow B850 excitation transfer to be of the order of picoseconds in *Rb. sphaeroides* and *Rps. acidophila* [5, 15]. Further studies with higher resolution measured the time scale to be ~ 0.8 - 0.9 ps for *Rps. acidophila* at room temperature, although, like most energy-transfer processes, this time scale is very temperature dependent. A longer B800 \rightarrow B850 excitation transfer time scale of 1.8-2.4 ps has been measured at 1.4-10 K [5].

The closest Mg-Mg distance between a B800 BChl and a B850 BChl is ~ 18 Å (you can check with VMD!), hence a pure Coulomb interaction picture as represented in Eqn. 4 is insufficient to describe the B800 \rightarrow B850 excitation transfer process. The time constant one calculates via the methods of Eqn. 4 and Eqn. 5 is necessarily longer than the actual time constant measured experimentally [5]. Another factor that should be considered when calculating B800 \rightarrow B850 time constant is the interaction between the Cars and the BChls. The close contact between Cars and both B800 and B850 BChls enables Cars to perturb the transition dipole moments of the BChls [3]. If such interaction is taken into account, the computed B800 \rightarrow B850 time constant can be improved to better agree with experiments [3].

6.5 B850 \leftrightarrow B850 excitation transfer

Upon looking at the organization of the B850 ring (as you have done in Exercise 5), one can deduce from the close nearest-neighbor distance of ~ 9 or ~ 9.5 Å that we need a better model to describe the excitation transfer process in the B850 ring than that provided by Eqn. 4 and Eqn. 5, which is only effective over a longer separation range. Also, a working model should incorporate the dimerized structure of the B850 ring. Therefore, an effective Hamiltonian formulation has been developed to describe the excitation transfer process within the B850 ring [3, 5, 12, 13, 17].

Under normal light conditions, bacterial LH-II receives a very low incoming light flux of about 10 photons per seconds per BChl [12]. This allows one to assume that, at any given time, only one BChl is excited to its lowest excitation state Q_y while all other BChls remain in ground state. Hence a reasonable choice of basis set for an effective Hamiltonian describing a ring of N-many B850 BChls can be expressed as:

$$|i\rangle = |\phi_1 \phi_2 \dots \phi_i^* \dots \phi_N\rangle, \quad i = 1, 2, \dots, N. \quad (6)$$

In this representation the i -th BChl is in its first excitation state ϕ_i^* , where all other BChls are in

their ground state. In this basis set an effective Hamiltonian can be expressed as

$$H = \begin{pmatrix} \epsilon_0 & W_{1,2} & W_{1,3} & \dots & \dots & W_{1,N-1} & W_{1,N} \\ W_{2,1} & \epsilon_0 & W_{2,3} & \dots & \dots & W_{2,N-1} & W_{2,N} \\ W_{3,1} & W_{3,2} & \epsilon_0 & \dots & \dots & W_{3,N-1} & W_{3,N} \\ \vdots & \vdots & \vdots & \vdots & \vdots & \vdots & \vdots \\ W_{N-2,1} & W_{N-2,2} & W_{N-2,3} & \dots & \epsilon_0 & W_{N-2,N-1} & W_{N-2,N} \\ W_{N-1,1} & W_{N-1,2} & W_{N-1,3} & \dots & W_{N-1,N-2} & \epsilon_0 & W_{N-1,N} \\ W_{N,1} & W_{N,2} & W_{N,3} & \dots & W_{N,N-2} & W_{N,N-1} & \epsilon_0 \end{pmatrix}. \quad (7)$$

Here ϵ_0 is the lowest excitation energy of each B800 BChl, and W_{ij} is the interaction energy between BChl i and j . One needs to treat each W_{ij} carefully due to the dimerized structure of B850 ring, since the nearest-neighbor interaction energy between two BChls with Mg-Mg spacing of $\sim 9\text{\AA}$ is different from the interaction energy between two BChls that are $\sim 9.5\text{\AA}$ apart. For this reason, we can replace all the nearest neighbor interaction energies $W_{i,i+1}$ by two variables ν_1 and ν_2 , for nearest neighbor spacings ~ 9 and $\sim 9.5\text{\AA}$, respectively. As for non-neighboring BChls, we will take advantage of their larger Mg-Mg distances and approximate their interaction energies with the Coulomb term H_{ij} described in Eqn. 4. Also, since the Coulomb interaction decreases quickly with large Mg-Mg distance r_{ij} , we can neglect interaction energies W_{ij} where $j > i+2 \pmod{N}$, namely, we will only consider nearest and next nearest neighbor interactions. After these treatments, the effective Hamiltonian for the B850 ring can be written as:

$$H = \begin{pmatrix} \epsilon_0 & \nu_1 & H_0 & \dots & \dots & H_0 & \nu_2 \\ \nu_1 & \epsilon_0 & \nu_2 & \dots & \dots & 0 & H_0 \\ H_0 & \nu_2 & \epsilon_0 & \dots & \dots & 0 & 0 \\ \vdots & \vdots & \vdots & \vdots & \vdots & \vdots & \vdots \\ 0 & 0 & 0 & \dots & \epsilon_0 & \nu_2 & H_0 \\ H_0 & 0 & 0 & \dots & \nu_2 & \epsilon_0 & \nu_1 \\ \nu_2 & H_0 & 0 & \dots & H_0 & \nu_1 & \epsilon_0 \end{pmatrix}. \quad (8)$$

The eigenvalues for Eqn. 8 is calculated to be [5]:

$$E_k = \epsilon_0 + 2H_0 \cos\left(\frac{2\pi k}{n}\right) \pm \sqrt{\nu_1^2 + \nu_2^2 + 2\nu_1\nu_2 \cos\left(\frac{2\pi k}{n}\right)}, \quad (9)$$

where the quantum number k denotes the excitation level of the B850 ring, and n is the number of BChl pairs, *i.e.* $n = N/2$. The allowed quantum numbers are $k = 0, \pm 1, \dots, \pm(n-1)/2$ if n is odd or $k = 0, \pm 1, \dots, \pm n/2$ if n is even. Hence, as we will see in Exercise 8, the effective Hamiltonian description predicts a spectrum of quantum states for the B850 BChl ring with energy level given by Eqn. 9.

Due to the strong coupling energy among the B850 BChls, excitation of one B850 travels to other B850 BChls at a very fast time scale of about 100-200 fs [15]. This feature is optimal for the excitation transfer from LH-II to LH-I, since such transfer is equally efficient from any of the B850 BChls.

Exercise 9: Excitation Spectrum of B850 Ring

1. Write out the allowed quantum number k for the *Rps. acidophila* B850 ring.
2. Write out the allowed energy level E_k for the *Rps. acidophila* B850 ring in terms of variables ϵ_0 , H_0 , ν_1 and ν_2 .
3. Sketch the energy levels E_k for the *Rps. acidophila* B850 ring.

References

- [1] R.E. Blankenship. Origin and early evolution of photosynthesis. *Photosyn. Res.*, 33:91–111, 1992.
- [2] J. Xiong, W. M. Fischer, K. Inoue, M. Nakahara, and C. E. Bauer. Molecular evidence for the early evolution of photosynthesis. *Science*, 289:1724–1730, 2000.
- [3] Xiche Hu, Thorsten Ritz, Ana Damjanović, Felix Autenrieth, and Klaus Schulten. Photosynthetic apparatus of purple bacteria. *Quart. Rev. Biophys.*, 35:1–62, 2002.
- [4] Miroslav Z. Papiz, Steve M. Prince, Tina Howard, Richard J. Cogdell, and Neil W. Isaacs. The structure and thermal motion of the B800-850 LH2 complex from *Rps. acidophila* at 2.0 Å resolution and 100K: New structural features and functionally relevant motions. *J. Mol. Biol.*, 326:1523–1538, 2003.
- [5] R. J. Cogdell, A. Gall, and J. Köhler. The architecture and function of the light-harvesting apparatus of purple bacteria: from single molecules to *in vivo* membranes. *Quart. Rev. Biophys.*, 39:227–324, 2006.
- [6] J. B. Arellano, B. B. Raju, K. R. Naqvi, and T. Gillbro. Estimation of pigment stoichiometries in photosynthetic systems of purple bacteria: special reference to the (absence of) second carotenoid in lh2. *Photochemistry and Photobiology*, 68:84–87, 1998.
- [7] Xiche Hu, Dong Xu, Kenneth Hamer, Klaus Schulten, Jürgen Koepke, and Hartmut Michel. Knowledge-based structure prediction of the light-harvesting complex II of *Rhodospirillum molischanum*. In P. M. Pardalos, D. Shalloway, and G. Xue, editors, *Global Minimization of Nonconvex Energy Functions: Molecular Conformation and Protein Folding*, pages 97–122. American Mathematical Society, Providence, R.I., 1996.
- [8] L. Janosi, H. Keer, I. Kosztin, and T. Ritz. Influence of subunit structure on the oligomerization state of light-harvesting complexes: a free energy calculation study. *Chemical Physics*, 323:117–128, 2005.
- [9] E. Roberts, J. Eargle, D. Wright, and Z. Luthey-Schulten. MultiSeq: Unifying sequence and structure data for evolutionary analysis. *BMC Bioinformatics*, 7:382, 2006.
- [10] Robert E. Blankenship. Molecular evidence for the evolution of photosynthesis. *Trends Plant Sci.*, 6:4–6, 2001.
- [11] Robert E. Blankenship. *Molecular Mechanisms of Photosynthesis*. Blackwell Science, Malden, MA, 2002.
- [12] Melih Şener and Klaus Schulten. Physical principles of efficient excitation transfer in light harvesting. In David L. Andrews, editor, *Energy Harvesting Materials*, pages 1–26. World Scientific, Singapore, 2005.
- [13] Klaus Schulten. From simplicity to complexity and back: Function, architecture and mechanism of light harvesting systems in photosynthetic bacteria. In H. Frauenfelder, J. Deisenhofer, and P. G. Wolynes, editors, *Simplicity and Complexity in Proteins and Nucleic Acids*, pages 227–253, Berlin, 1999. Dahlem University Press.

- [14] Thorsten Ritz, Ana Damjanović, and Klaus Schulten. The quantum physics of photosynthesis. *ChemPhysChem*, 3:243–248, 2002.
- [15] V. Sundström, T. Pullerits, and R. van Grondelle. Photosynthetic light-harvesting: Reconciling dynamics and structure of purple bacterial LH2 reveals function of photosynthetic unit. *J. Phys. Chem. B*, 103:2327–2346, 1999.
- [16] D.L. Dexter. A theory of sensitized luminescence in solids. *J. Chem. Phys.*, 21:836–850, 1953.
- [17] Xiche Hu, Thorsten Ritz, Ana Damjanović, and Klaus Schulten. Pigment organization and transfer of electronic excitation in the purple bacteria. *J. Phys. Chem. B*, 101:3854–3871, 1997.